

Moustakas-AK; Routsias-JG; Papadopoulos-GK *Structural modelling I-A^{g7} of NOD mouse: Μοντελοποίηση των MHC II αλληλίων του I-Ag7 των NOD ποντικών: η εξαρτώμενη από το pH ειδικότητα στις θέσεις 9 και 6 εξηγεί αρκετές από τις ιδιαιτερότητες των μορίων αυτών*. Diabetologia. 1995 Nov; 38(11): 1251-61.

Το NOD διαβητικό ποντίκι είναι ένα ζώο-μοντέλο του ινσουλινοεξαρτώμενου νεανικού διαβήτη. Το κύριο γενετικό χαρακτηριστικό του είναι ένα μοναδικό αλληλίο MHC τάξεως II το οποίο ονομάζεται I-A^{g7}. Ο σκοπός της μελέτης αυτής ήταν να δημιουργηθεί ένα τρισδιάστατο μοντέλο της δομής του I-A^{g7} και να μελετηθούν τα ασυνήθιστα δομικά χαρακτηριστικά του. Η μοντελοποίηση του αλληλίου αυτού σε σύμπλεξη με γνωστά αντιγονικά πεπτίδια, βασίστηκε στη δομή του I-A^k και πραγματοποιήθηκε με τη βοήθεια ειδικού λογισμικού μοριακής μοντελοποίησης (InsightII και Discover). Όταν το μόριο I-A^{g7} μεταπίπτει από pH=5 των ενδοσωμάτων στο pH=7 του εξωκυττάρου χώρου, η εκλεκτικότητα του μεταβάλλεται δραματικά στις θέσεις αγκίστρωσης 9 και 6, αλλά πολύ λίγο στις θέσεις πρόσδεσης 1, 4 και 7, γεγονός που βρίσκεται σε συμφωνία με προηγούμενες μελέτες. Η εκλεκτικότητα αυτή οφείλεται στο μοναδικό συνδυασμό των β9 His, β5 His και β57 Ser. Στο pH=5 τα θετικά φορτία, μέσα και γύρω από τη θέση αγκίστρωσης 9, ευνοούν τη σύνδεση με αρνητικά φορτισμένα κατάλοιπα. Στο pH=7 όμως, οι αφόρτιστες ιστιδίνες α68, β9 και β56 ευνοούν την υποδοχή ογκωδών καταλοίπων, όπως η λυσίνη, αργινίνη, φαινυλανανίνη και η τυροσίνη, στη θέση αγκίστρωσης 9. Επίσης, εξαρτώμενη από το pH εκλεκτικότητα παρατηρείται και στη θέση αγκίστρωσης 6 και οφείλεται στο συνδυασμό β9 His και α66 Glu. Επιπλέον η έλλειψη απόθησης ανάμεσα στη β56 His και α76 Arg στο pH=7 οδηγεί σε αποσταθεροποίηση της τριτοταγούς δομής. Τα αποτελέσματα αυτά αποσαφηνίζουν προηγούμενες ασυμφωνίες για τα πεπτίδια που δεσμεύει το I-A^{g7} και τα μοτίβα των αμινοξέων τους. Επιπλέον παρέχονται πιθανές εξηγήσεις (α) για το μικρό in vivo χρόνο ζωής των μεμβρανικών συμπλόκων I-A^{g7}, (β) την αποτελεσματικότερη αρνητική επιλογή στο θύμο και την έμφυτη αυτοδραστικότητα των ανοσοκυττάρων που εμφανίζεται στα ποντίκια αυτά και (γ) την προστασία από τον διαβήτη που παρέχεται στα συγκεκριμένα ζώα από την έκφραση τροποποιημένων I-A^{g7} μορίων ή άλλων αλληλίων MHC τάξεως II.

Οι παρατηρήσεις αυτές συμβάλλουν στην κατανόηση της παθογένεσης του τύπου I ινσουλινοεξαρτώμενου διαβήτη στα ποντίκια NOD.

Modelling of the MHC II allele I-A^{g7} of NOD mouse: pH-dependent changes in specificity at pockets 9 and 6 explain several of the unique properties of this molecule

A. K. Moustakas¹, J. Routsias^{2,3}, G. K. Papadopoulos¹

¹ Laboratory of Biochemistry and Biophysics, Faculty of Agricultural Technology, Technological Educational Institute of Epirus, Arta, Greece

² Laboratory of Immunology, Department of Internal Medicine, University of Ioannina Medical School, Ioannina, Greece

³ Current address: Laboratory of Pathophysiology, Medical School University of Athens, Athens, Greece

Abstract

Aims/hypothesis. We modelled the three-dimensional structure of I-A^{g7}, the chief genetic component of diabetes in non-obese diabetic mice, to understand the unusual properties of this molecule.

Methods. Modelling was done, in complex with established antigenic peptides, based on the structure of I-A^k.

Results. The selectivity of the I-A^{g7} molecule changes greatly at pockets 9 and 6 but hardly at all at pockets 1, 4 and 7, between endosomal pH (5.0) and extracellular pH (7.0), in agreement with previous results. This selectivity is attributed to the unique combination of β9His, β56His and β57Ser. The positive charges in and around pocket 9 at pH 5, favour binding by negatively charged residues. At pH 7 however, the uncharged α68, β9 and β56 histidines favour the accommodation of the bulky residues lysine, arginine, phenylalanine and tyrosine at pocket 9. The combina-

tion of β9His and α66Glu is responsible for the pH-dependent selectivity at pocket 6. Furthermore, the lack of repulsion between β56His and α76Arg at pH 7 leads to a more stable ternary complex.

Conclusion/interpretation. These results reconcile previous conflicts over the peptide binding ability of I-A^{g7} and its motif. They furthermore provide possible explanations for the short lifetime of cell-surface I-A^{g7} complexes in vivo, the higher threshold of thymic negative selection and inherent self-reactivity shown by immunocytes in these mice and the protection from diabetes afforded to them by several transgenically expressed mouse class II alleles. This contributes to an understanding of the pathogenesis of Type I (insulin-dependent) diabetes mellitus in this animal. [Diabetologia (2000) 43: 609–624]

Keywords Autoimmunity, I-A^{g7} molecule, MHC class II structure, protein modelling, NOD mice, Type I diabetes mellitus.

The non-obese diabetic (NOD) mouse is an animal model of Type I (insulin-dependent) diabetes mellitus [1, 2]. Extensive work on this model has shown

Received: 9 August 1999 and in revised form: 27 January 2000

Corresponding author: G. K. Papadopoulos, PhD, Laboratory of Biochemistry and Biophysics, Faculty of Agricultural Technology, Technological Educational Institute of Epirus, GR-47100 Arta, Greece

Abbreviations: aa, Amino acid; APC, antigen-presenting cell; CLIP, class II associated invariant chain peptide; GAD, glutamic acid decarboxylase; HEL, hen egg white lysozyme; hsp60, heat-shock protein 60; IC₅₀, concentration yielding 50% inhibition in competitive binding experiments using soluble I-A^{g7}; NOD, non-obese diabetic; p, pocket, position.

that the chief genetic determinant of diabetes is the unique MHC class II allele of this mouse, termed I-A^{g7} [2, 3]. The MHC class II molecules exist on professional antigen-presenting cells (APCs, i. e. dendritic cells, B lymphocytes and macrophages). They capture processed antigen fragments, forming complexes that are presented to CD4⁺ helper T-cells. Because of a deletion in their *H-2/I-Eα* gene, NOD mice do not express an I-E molecule [4]. Sequencing of the I-A^{g7} molecule showed a number of remarkable features in its beta chain; a histidine in position 56 and a serine in position 57 [5]. The histidine is unique to I-A^{g7} of all known mouse, rat, porcine, bovine and human MHC class II alleles [6, 7]. The β57Ser is unique to the I-A^{g7} of all mouse MHC class II alleles but is

also found in a number of such alleles in rat and humans [6]. Specifically in humans, the $\beta 57$ position is polymorphic and has been identified early on as one of the key determinants of diabetes susceptibility, which is associated with the absence of aspartate in susceptible HLA-DQ alleles [8]. The alpha chain of I-A^{g7} is identical to that of I-A^d [1, 4].

Establishing the three-dimensional structure of seven different MHC class II alleles, DR1, DR2, DR3, DR4, I-E^k, I-A^d and I-A^k, each in complex with an antigenic peptide, has allowed the delineation of the binding rules and motifs of antigenic peptides to such molecules [9–15]. The overall shape of mouse and human MHC class II alleles is very similar. In the antigen-binding domain, $\alpha 1\beta 1$, the binding groove is formed by two antiparallel α -helical “walls” to either side of a β -pleated sheet floor. The antigenic peptide fits into the groove with its backbone nearly parallel to the axes of the α -helical walls and its amino and carboxy termini projecting out of the two openings of the groove. The specificity in the binding of various residues of the antigenic peptide is provided by several depressions in the antigen-binding groove, termed “pockets”. The binding and crystallographic data show unequivocally that in human HLA-DR molecules, and their mouse counterparts H-2/I-E, the pockets for the binding of residues from the antigenic peptide occur at relative positions 1, 4, 6, 7 and 9, designated as pocket (p)1, p4 etc. [16]. Bound peptides isolated from MHC II molecules can be 11–22 residues long, containing the nonamer core flanked by a few to several amino acids on either side [16]. The non-specific mode of peptide binding is facilitated by the several strategically positioned polar residues. Many of them are invariant and mostly they are from the $\alpha 1$ and $\beta 1$ helices that form hydrogen bonds to select amide and carbonyl groups of the bound antigenic peptide. The only structural features unique to mouse I-A alleles occur in the $\alpha 1\beta 1$ antigen binding domain; a β -bulge at position $\alpha 9$ and an amino acid insertion at $\beta 84$ a (for an explanation of notation see Materials and methods and Fig. 1), 10 residues earlier than assumed previously [6, 14, 15, 17].

Contrasting findings by several laboratories range from the unique I-A^{g7} molecule being a poor [18] or a good binder [19–27] of antigenic peptides with sharply varying specificities at pockets 6 and 9 [21–23]. One study found purified I-A^{g7} to be a very weak binder of several antigenic peptides at pH 5.5 [18] but three other studies done at pH 4.5 to 5.5 and using mostly different peptides, reported binding affinities in the low to mid- $\mu\text{mol/l}$ range [24–26]. Another study tested binding at pH 5 of peptide 12 from mouse heat-shock protein 60 (hsp60) to activated, and then paraformaldehyde-fixed, peritoneal macrophages of NOD mice, thus deriving a motif for the various pockets of the I-A^{g7} allele [21]. In a subsequent binding/stability study, also at pH 5, the same

group reported similar results [23]. By contrast, binding of the immunogenic [28] hen egg white lysozyme (HEL) 10–22 peptide and several of its variants to purified I-A^{g7} molecules was tested in another study at pH 7, where a higher affinity [concentration for 50% inhibition of binding (IC_{50}) = 295 nmol/l] for the peptide and a different motif were established [22]. These peptides were also tested for activation of a HEL10–22-specific, I-A^{g7}-restricted T-cell hybridoma [22]. The stability of I-A^{g7} molecules in vivo [18, 21, 23, 29–31] and in vitro [21–23, 26] has also been variably reported by different groups, either as very low in vivo [18, 29–31] and in vitro [18, 26], or high in vivo [21, 23]. We have taken into account the results of these binding studies at different pH values and carried out homology modelling of I-A^{g7} complexed to this antigenic peptide from HEL, as well as to established epitopes of the primary autoantigen glutamic acid decarboxylase (GAD) [24, 25, 32–42], the GAD homologous peptide from the C2 protein of Coxsackie B4 viral strain [43], the autoantigens insulin beta chain [44, 45] and hsp60 peptide 12 [21, 23], antigenic peptides from sperm whale, equine, and mouse myoglobins [46, 47], class II invariant chain peptide (CLIP) and I-A^{g7}-derived and I-E α -derived immunogens [25–27], carboxypeptidase H [18, 26] and two I-A^{g7}-eluted peptides derived from mouse serum albumin and transferrin [19, 26].

Materials and methods

Coordinates of crystal structure, I-A^{g7} and peptide alignments and amino acid conformations for modelling. The coordinates of the I-A^k complexed to the HEL50–62 peptide [14] were obtained from Dr. D. Fremont and the Protein Data Bank (access code 1iak). They include the positions of residues 1–181 of the alpha chain and 5–190 of the beta chain as well as the coordinates of the bound HEL50–62 peptide and those of the linker peptide connecting the carboxy-terminus of the HEL peptide to the amino terminus of the beta chain. The alignment of I-A^{g7} and I-A^k molecules was done as in [14]. (See also Fig. 1 of this work). The numbering scheme used for the alpha and beta chains of I-A^{g7} was identical to the one adopted by these authors. Modelling work was done on an Indy computer workstation (Silicon Graphics, Mountain View, Calif., USA) using the programs Insight II/Discover, versions 95.0/2.9.7/3.0 (Biosym Technologies/Molecular Simulations, San Diego, Calif., USA). The I-A^{g7} alpha chain is 87% identical to the I-A^k alpha chain in the $\alpha 1$ domain, and 97% identical in the $\alpha 2$ domain. The I-A^{g7} β chain is 88% identical to the I-A^k beta chain in the $\beta 1$ domain and 96% identical in the $\beta 2$ domain, a much higher homology than shown to DR1 [48]. There were no amino acid substitutions in the sequence that would be expected to greatly change the local secondary structure of I-A^{g7}. The individual amino acid conformations were automatically chosen by the modelling program from a library of rotamers contained in it, using the most suitable rotamer for each case. The antigenic peptides used to occupy the respective positions in the groove were those reported as immunogenic in NOD mice, either in spontaneous or induced responses [21–28, 32–47].



Fig. 1A, B. Amino acid sequences of the alpha (**A**) and beta (**B**) chains of the mouse I-A^d, I-A^k and I-A^{g7} alleles and DR1 in the $\alpha 1\beta 1$ domain. The numbering used in the alpha chain and the beta chain is that proposed previously [14]. Code: .: Identity; -: no amino acid in corresponding position (specifically, $\alpha 9a$ and $\beta 84a$); !: intermolecular hydrogen bonds between MHC class II molecule and the bound antigenic peptide; *: residues forming p1; ^: residues forming p4; &: residues forming p6; |: residues forming p7; \$: residues forming p9. ^aIn DR, $\alpha 7Ile$ is part of p1 whereas in I-A alleles the equivalent residue is $\alpha 9Tyr$. ^b $\alpha 52$ and $\alpha 54$ are part of p1 only in I-A alleles. In I-A^k alone $\alpha 53$ is also part of p1. ^cIn I-A^{g7}, modelling shows the $\beta 30$ and $\beta 37$ Tyr residues to participate in p9 when this pocket is occupied by Arg/Lys/Phe/Tyr at pH 7. ^dIn I-A^{g7}, modelling shows that $\beta 61Tyr$ participates in the formation of both p7 and p9. ^eIn I-A^{g7}, modelling shows that $\beta 70Arg$ and $\beta 71Thr$ participate in the formation of p7, while in DR1, $\beta 71Arg$ is part of both pockets 4 and 7 and $\beta 70Gln$ is part of pocket 4 only. In the crystal structure of I-A^k both residues are part of p7 while in the crystal structure of I-A^d, $\beta 71Thr$ is part of p7 and $\beta 70Arg$ does not seem to participate in the formation of either pocket

The ionisation state of amino acid side-chains was that at pH 5, the approximate pH of the endosomal compartment or pH 7. The register for fitting each peptide into the groove was resolved by using the results of the extensive peptide competition binding studies to I-A^{g7} at pH 5 and pH 7 [21, 22]. The respective motifs are called by us, but not by the authors of these works, “pH 5 motif” and “pH 7 motif”. The respective regis-

ters for fitting the antigenic peptides at each pH into the groove were decided by us on the basis of the motif studies (Table 1). Energy minimisation of the I-A^{g7}-peptide complexes was done for most peptides in at least two different registers and at two different pH values (5 and 7). As the I-A^k-HEL50–62 coordinates included a 13-mer peptide, all peptides used in the energy minimisation studies (except known cases of tested shorter peptides) included a nonamer core (p1-p9) and, wherever possible, two residues on either side of the core amino termini and carboxy termini.

The ionisation state of the three histidines ($\alpha 68$, $\beta 9$ and $\beta 56$) in and around p9 at the two pH values, was decided as follows: at pH 5, $\alpha 68His$ and $\beta 56His$ are completely exposed to solvent and $\beta 9His$, although at the bottom of p9, can still come in contact with the solvent, when an acidic residue is at p9 (see Results). The crystal structures of I-A^k/I-A^d show that there is ample room between the p9Ser/Ala residue and $\beta 9His$ /Val respectively for at least two solvent molecules to interpose [14, 15]. Thus $\beta 9His$ of I-A^{g7} could be in contact with bulk solvent. Therefore, $\beta 9His$ will be 90% uncharged at pH 7 ($pK_a = 6.0$).

Energy minimisation. Energy minimisation was accomplished by the steepest gradient method first, followed by the conjugate gradient method provided by the program Discover. The minimisation procedure went through 1000 cycles for each method. In the first 50 to 100 cycles of each minimisation the energy of the molecule dropped considerably but by the end of each run there were only very small changes in the energy values. Extending the number of steps in the conjugate gradient stage to 10 000 for a number of I-A^{g7}-peptide complexes

Table 1. Minimised energy values for I-A^{g7}-antigenic peptide complexes at pH 5 and pH 7 in registers fulfilling each motif

| Name of antigen and/or peptide designation/peptide sequence | Amino acid sequence and register of binding 1 4 6 7 9 | Motif pH | Minimised Energy at | | References where given peptide is shown to be antigenic for the NOD mouse ^a |
|---|--|----------|---------------------|------|--|
| | | | pH 5 kcal/mol | pH 7 | |
| <i>HEL</i> | | | | | [22 ^b , 28] |
| 8–20 | L A A A M K R H G L D N Y | 5.0 | 1510 | 1493 | |
| 10–22 | A A M K R H G L D N Y R G | 7.0 | 1510 | 1414 | |
| 10–22p9F | A A M K R H G L D N F R G | " | | 1426 | |
| 10–22p9K | A A M K R H G L D N K R G | " | | 1416 | |
| 10–22p9R | A A M K R H G L D N R R G | " | | 1377 | |
| 10–22p9W | A A M K R H G L D N W R G | " | | 1465 | |
| 10–22p9A | A A M K R H G L D N A R G | " | | 1442 | |
| 10–22p9L | A A M K R H G L D N L R G | " | | 1441 | |
| 10–22p6M | A A M K R H G M D N Y R G | 7.0 | | 1406 | |
| 10–22p6I | A A M K R H G I D N Y R G | " | | 1416 | |
| 10–22p6V | A A M K R H G V D N Y R G | " | | 1417 | |
| 10–21 | A A M K R H G L D N Y R | 7.0 | | 1455 | |
| 10–20 | A A M K R H G L D N Y | " | | 1464 | |
| 10–19 | A A M K R H G L D N | " | | 1459 | |
| 10–18 | A A M K R H G L D | " | | 1488 | |
| 10–17 | A A M K R H G L | " | | 1507 | |
| 10–16 | A A M K R H G | " | | 1511 | |
| 10–15 | A A M K R H | " | | 1520 | |
| 11–22 | A M K R H G L D N Y R G | " | | 1436 | |
| 12–22 | M K R H G L D N Y R G | " | | 1441 | |
| 13–22 | K R H G L D N Y R G | " | | 1456 | |
| 14–22 | R H G L D N Y R G | " | | 1508 | |
| 15–22 | H G L D N Y R G | " | | 1482 | |
| 16–22 | G L D N Y R G | " | | 1489 | |
| 17–22 | L D N Y R G | " | | 1493 | |
| <i>Murine hsp60</i> | | | | | [21, 23] |
| Peptide 12 | | | | | |
| 169–181 | A Q V A T I S A N G D K D | 5.0 | 1501 | 1480 | |
| 169–181p9A | A Q V A T I S A N G A K D | " | 1515 | | |
| 169–181p9M | A Q V A T I S A N G M K D | " | 1510 | | |
| 169–181p6E | A Q V A T I S E N G D K D | " | 1411 | | |
| 169–181p6T | A Q V A T I S T N G D K D | " | 1448 | | |
| 169–181p7R | A Q V A T I S A R G D K D | " | 1440 | | |
| 169–180 | A Q V A T I S A N G D K | 5.0 | 1504 | | |
| 170–180 | Q V A T I S A N G D K | " | 1521 | | |
| 169–180p-2K | K Q V A T I S A N G D K | " | 1546 | | |
| 169–180p1A | A Q A A T I S A N G D K | " | 1490 | | |
| 169–180p1E | A Q E A T I S A N G D K | " | 1471 | | |
| 169–180p10A | A Q V A T I S A N G D A | " | 1474 | | |
| 169–180p9Y | A Q V A T I S A N G Y K | " | 1521 | | |
| Peptide 437–460 | | | | | |
| 449–460 | P A L D S L K P A N E D | 5.0 | 1447 | 1504 | |
| <i>Human hsp60</i> | | | | | [21, 23] |
| Peptide 449–460 | | | | | |
| 449–460 | P A L D S L T P A N E D | 5.0 | 1461 | 1483 | |
| <i>Murine GAD65</i> | | | | | [40] |
| Peptide 14 (aa202–221) | | | | | |
| 207–219 | Y E I A P V F V L L E Y V | 5.0 | 1564 | 1609 | |
| 208–220 | E I A P V F V L L E Y V T | 7.0 | 1612 | 1631 | |
| Peptide 15 (aa217–236 or 221–235) ^c | | | | | |
| 216–228 | L E Y V T L K K M R E I I | 5.0 | 1545 | 1545 | [24, 38, 40] |
| 217–227 | E Y V T L K K M R E I | 7.0 | 1585 | 1532 | |
| 221–232 | L K K M R E I I G W P G | " | 1627 | 1622 | |
| Peptide 17 (aa247–266) | | | | | |
| 254–266 | A R Y K M F P E V K E K G | 5.0 | 1538 | 1526 | [33, 42, 43] |
| 255–267 | R Y K M F P E V K E K G M | 7.0 | 1672 | 1643 | |
| 253–265 | I A R Y K M F P E V K E K | " | 1661 | 1674 | |
| Peptides 286–300 (aa286–300) and 290–309 (p290) | | | | | |
| 287–299 | K G A A A L G I G T D S V | 5.0 | 1515 | 1549 | [24, 42] |
| 295–307 | G T D S V I L I K C D E R | " | 1503 | 1498 | |
| 296–308 | T D S V I L I K C D E R G | " | 1401 | 1432 | |
| 293–305 | G I G T D S V I L I K C D | 7.0 | 1557 | 1520 | |
| 297–309 | D S V I L I K C D E R G K | " | 1745 | 1715 | |
| Peptide 401–415 | | | | | |
| 401–413 | P L Q C S A L L V R E E G | 5.0 | 1438 | 1454 | [24] |
| 402–414 | L Q C S A L L V R E E G L | " | 1423 | 1474 | |
| 401–412 | P L Q S S A L L V R E E | 7.0 | 1660 | 1658 | |

Table 1. Continued

| Name of antigen and/or peptide designation/peptide sequence | Amino acid sequence and register of binding 1 4 6 7 9 | Motif pH | Minimised Energy at | | References where given peptide is shown to be antigenic for the NOD mouse ^a |
|---|--|------------|---------------------|------|--|
| | | | pH 5 kcal/mol | pH 7 | |
| Peptide 34 (aa509–528) | | | | | [33, 35, 36, 39, 41] |
| 507–519 | WF V P P S L R T L E D N | 5.0 | 1573 | 1568 | |
| 508–520 | F V P P S L R T L E D N E | " | 1470 | 1521 | |
| 510–522 | P P S L R T L E D N E E R | " | 1358 | 1418 | |
| 511–523 | P S L R T L E D N E E R M | " | 1382 | 1429 | |
| 512–524 | S L R T L E D N E E R M S | 7.0 | 1592 | 1610 | |
| Peptide 35 (aa524–543) | | | | | [33, 37, 39, 41] |
| 529–541 | V A P V I K A R M M E Y G | 5.0 | 1581 | 1564 | |
| 528–540 | K V A P V I K A R M M E Y | " | 1647 | 1671 | |
| 524–536 | S R L S K V A P V I K A R | 7.0 | 1654 | 1599 | |
| 526–538 | L S K V A P V I K A R M M | " | 1861 | 1814 | |
| 530–542 | A P V I K A R M M E Y G T | " | 1556 | 1542 | |
| Peptide 36 (aa539–558) | | | | | [33] |
| 542–554 | T T M V S Y Q P L G D K V | 5.0 | 1593 | 1601 | |
| 545–557 | V S Y Q P L G D K V N F F | " | 1620 | 1646 | |
| 537–549 | M M E Y G T T M V S Y Q P | 7.0 | 1600 | 1619 | |
| Peptide 561–575 | | | | | [24] |
| 561–572 | I S N P A A T H Q D I D | 5.0 | 1461 | 1524 | |
| 562–574 | S N P A A T H Q D I D F L | " | 1490 | 1543 | |
| 563–575 | N P A A T H Q D I D F L I | 7.0 | 1533 | 1514 | |
| <i>B4 Coxsackie virus, C-2 protein</i> | | | | | [43] |
| 32–47 | L K V K I L P E V K E K H | 5.0 | 1675 | 1637 | |
| 33–45 | K V K I L P E V K E K H E | 7.0 | 1639 | 1610 | |
| <i>Murine insulin</i> | | | | | [44, 45] |
| B11–23 | L V E A L Y L V C G E R G | 5.0 | 1458 | 1464 | |
| B12–24 | V E A L Y L V C G E R G F | 7.0 | 1573 | 1578 | |
| <i>Murine Ii (88–100)</i> | | | | | [26] |
| CLIP | S Q M R M A T P L L M R P | 5.0 or 7.0 | 1544 | 1501 | |
| <i>Murine serum albumin</i> | | | | | [19, 26] |
| 563–574 | A T A E Q L K T V M D D | 5.0 | 1413 | 1538 | |
| <i>Murine transferrin</i> | | | | | [19, 26] |
| 57–68 | N Y V T A I R N Q O E G | 5.0 | 1400 | 1466 | |
| 55–65 | G H N Y V T A I R N Q | 7.0 | 1755 | 1721 | |
| <i>Murine MHC II peptides</i> | | | | | [19, 25, 27] |
| I-A ^{g7} β87–97 | V P T S L R R L E Q P | 5.0 | 1455 | 1434 | |
| I-Eα 48–58 | F A K F A S F E A Q | 5.0 | 1623 | 1603 | |
| I-Eα 54–68 | F E A Q G A L A N I A V D K A | 5.0 | 1500 | 1523 | |
| I-Eα all Ala anchors | A E A A A A L A A I A A A A A | 5.0 | 1541 | 1506 | |
| Scrambled peptide ^d | V N Q S L R P T P L E I S | 5.0 | 1449 | | |
| <i>Human Carboxypeptidase H 362–382</i> | | | | | [18, 26] |
| 362–372 | K N S L I N Y L E Q I | 5.0 | 1468 | 1502 | |
| 369–381 | L E Q I H R G V K G F V R | 7.0 | 1634 | 1636 | |
| <i>Myoglobin</i> | | | | | [46, 47] |
| Equine 69–78 | L T A L G G I L K K | 7.0 | 1633 | 1614 | |
| Equine 69–78 ^e | L T A L G G I L K K | " | 1633 | 1599 | |
| Mouse 69–78 | L T A L G T I L K K | 7.0 | 1671 | 1604 | |
| Mouse 69–78 ^e | L T A L G T I L K K | " | 1633 | 1591 | |
| Sperm whale 108–120 | S E A I I H V L H S R H P | 7.0 | 1901 | 1799 | |
| Sperm whale 110–120 | A I I H V L H S R H P | " | 1728 | 1837 | |
| Mouse 110–120 | I I I E V L K K R H S | 7.0 | 1856 | 1771 | |
| Mouse 110–119 | I I I E V L K K R H | " | 1748 | 1587 | |

^a References here denote sources where these peptides were shown to be antigenic. Reference 21 also contains a table aligning known immunogenic for the NOD mouse peptides in the register fulfilling the motif found by these workers (i.e. pH 5) and reference 22 makes extensive use of substitutions to verify its motif (pH 7)

^b The HEL 10–22 peptide is the only one from the list above that has had characterisation of its binding affinities by extensive substitution at each position, as reported [22]

^c Reference 38 tested peptide 221–235, in which only the 12-mer 221–232 could bind in the pH 7 motif register with 222K as p1 anchor and reference 40 tested the sequence 217–236 which contains the 217–227 11-mer with 217E as p1 anchor

^d Control peptide for first two peptides in the series [25]

^e Alternative register of same sequence

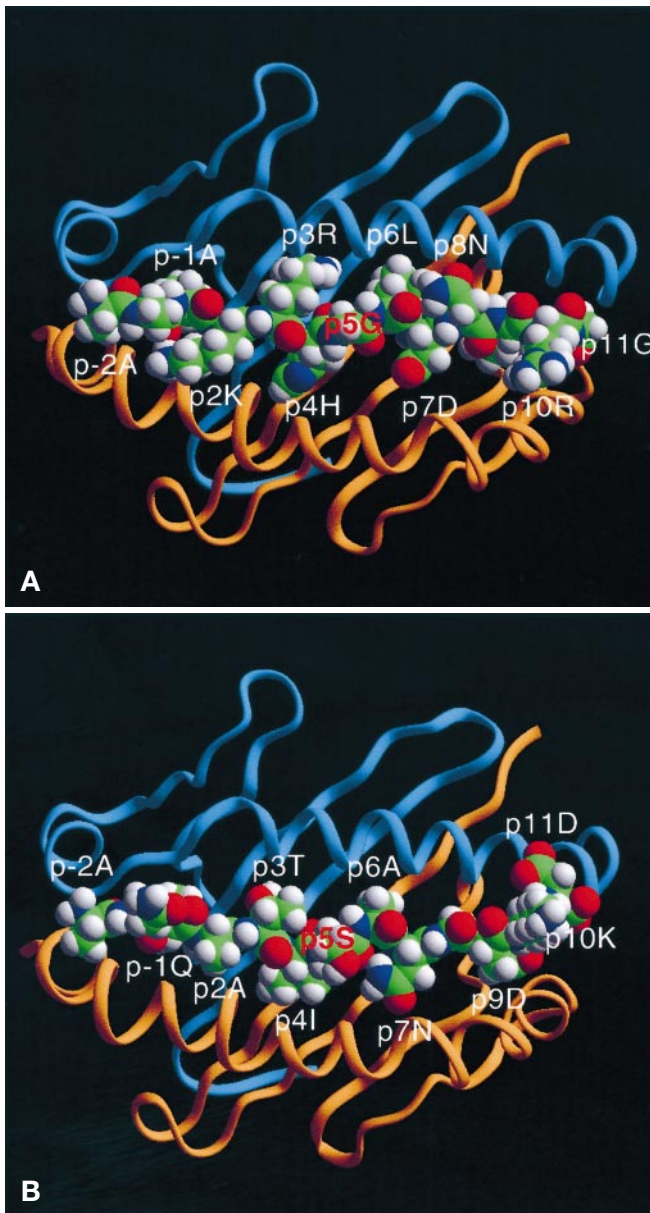


Fig. 2 A, B. Three-dimensional structure of the modelled $\alpha 1\beta 1$ domain of I-A^{g7}, complexed (**A**) with the HEL10–22 peptide (p1 as 12Met) at pH 7 and (**B**) with the mouse hsp60 peptide 12 at pH 5 (alpha and beta chains in ribbon form) as viewed from “above” (T-cell receptor view). The $\alpha 1$ domain is in light blue, the $\beta 1$ domain is in brick red and the antigenic peptide residues are in space-filling form. The orientation and hydrogen bonding distances were essentially the same for the various peptides modelled, regardless of the pH value. Carbon: green, oxygen: red, nitrogen: blue, hydrogen: white, sulphur: yellow

produced a reduction in total energy by about 2.5% with no cross-overs in the energy differences among the different complexes. The consistent valence force field of Discover was used, which included electrostatic terms for interactions up to 16 Å. A simple harmonic potential rather than a Morse potential was used and no cross-terms were included. The dielectric constant used was 1/r. No account was taken of the water molecules. The coordinates of the I-A^{g7} complexed to peptide 12

Table 2. Groups from $\alpha 1\beta 1$ of I-A^{g7} that participate in hydrogen bonds to the antigenic peptide backbone^a

| I-A ^{g7} group | Peptide backbone group | Equivalent hydrogen bond found in ^b | |
|--------------------------------|------------------------|--|------------------|
| | | I-A ^k | I-A ^d |
| $\alpha 51$ N | p-2 NH | No | No |
| $\alpha 53$ N | p-2 O | Yes | Yes |
| $\beta 81$ His N ϵ 2 | p-1 O | Yes | Yes |
| $\alpha 53$ O | p1 NH | Yes | Yes |
| $\beta 82$ Asn O δ 1 | p2 NH | Yes | Yes |
| $\beta 82$ Asn N δ 2 | p2 O | Yes | Yes |
| $\alpha 24$ His N ϵ 2 | p2 O | NA ^c | No |
| $\alpha 9$ Tyr O η | p4 NH | Yes | Yes |
| $\alpha 62$ Asn N δ 2 | p4 O | No | Yes |
| $\beta 74$ Glu O ϵ 2 | p5 NH | Yes | Yes |
| $\beta 70$ Arg N η 2 | p5 O | No | No |
| $\alpha 11$ Thr O γ | p5 O | No | No |
| $\alpha 62$ Asn O δ 1 | p6 NH | Yes | Yes |
| $\beta 30$ Tyr O η | p7 NH | Yes | Yes |
| $\alpha 69$ Asn N δ 2 | p7 O | Yes | Yes |
| $\beta 67$ Tyr O η | p8 NH | No | NA ^d |
| $\beta 61$ Tyr O η | p8 O | No ^e | Yes ^e |
| $\alpha 69$ Asn O δ 1 | p9 NH | Yes | Yes |
| $\alpha 68$ His N ϵ 2 | p9 O | Yes | Yes |

^a No account is taken of hydrogen bonds between side-chains of the protein and the antigenic peptide

^b Data obtained by inspection of the deposited coordinates

^c Not applicable, I-A^k has a Phe at this position

^d I-A^d has a Glu at this position

^e I-A^d and I-A^k have a Trp at this position

of hsp60 at pH 5, and to the HEL10–22 peptide at pH 7, will be deposited in the Protein Data Bank and in the meantime are available from the authors.

Results

Overall structural features. We put 93 different peptide sequences in complex with I-A^{g7} through the energy minimisation process, at pH 5 or pH 7 or both for a total of 158 minimisations (Table 1). The resulting I-A^{g7} molecule, whether at pH 5 or at pH 7, shows very little deviation in its secondary, tertiary and quaternary structure from that of I-A^k. Figure 2 shows the overall shape of the $\alpha 1\beta 1$ domain of the I-A^{g7} molecule in complex with peptide 12 of mouse hsp60 protein (at pH 5) and with HEL10–22 (at pH 7). Hydrogen bonds with the amide and carbonyl groups of the bound peptide are formed by the same or equivalent polar residues in the $\alpha 1\beta 1$ domain as in I-A^d and I-A^k (Fig. 1, 2; Table 2). The orientation of the backbones of the antigenic peptides is nearly identical to that of HEL50–62 in I-A^k, i.e. they have a downward bend at the centre, because of $\beta 13$ Gly.

Energy minimisation. We first tested whether the minimisation procedure would reliably predict the better binding peptides as those resulting in lower to-

tal energies of I-A^{g7}-peptide complexes. Thus we did the minimisation of the I-A^{g7}-peptide complexes of HEL10–22 and hsp60 peptide 12 and several of their truncated or substituted variants (one deletion or substitution at a time) because quantitative and semi-quantitative results of *in vitro* binding studies respectively were available for comparison [21–23]. Only in 3 out of 12 cases the energy of the I-A^{g7}-hsp60 peptide 12 variant complex did not correlate with reported binding, or lack of, to I-A^{g7}: in p1E the energy was lower than that of the reference peptide-I-A^{g7} complex, instead of the expected higher value and in p6T and p6E, the energies were lower instead of slightly higher than that of the same reference value (Table 1; [21, 23]). Likewise, there was very good correlation in 19 out of 22 cases between the energies of the substituted and truncated HEL10–22 peptides with I-A^{g7} in the pH 7 register and the experimentally derived affinities to this allele (discordant peptides 11–22, 12–22 and 13–22, Table 1, [22]); a plot of total energy against log IC₅₀ for the HEL peptides yielded a linear result (data not shown). We observed no statistically significant energy differences among different preferred residues in pockets 1, 4 and 7 between pH values of 5 and 7 (data not shown). Thus, any pH-dependent motif differences at these pockets are very small. A standard deviation of 5.2 kcal/mol was obtained from the repeated (ten times) minimisation, starting from a different atom each time, of the I-A^{g7}-HEL10–22 complex at pH 7. Therefore, we consider energy differences of ± 13.2 kcal/mol (± 2.54 SD) as significant ($p < 0.01$).

A comparison of energy values can be made for the same I-A^{g7}-peptide complex at two different pH values. Likewise, the deletion, addition or substitution of one residue to a peptide “bound” to I-A^{g7} can be compared with the “native” peptide bound in the same register. Comparisons of the minimised energy of different peptide-I-A^{g7} complexes, when the peptide sequences bear no relation to each other, have little meaning. Furthermore, as these minimisations do not consider possible interactions with water molecules, no correlation between the total energy of the various I-A^{g7}-peptide complexes and their respective dissociation constants can be made.

Table 1 shows the total energy values obtained for several I-A^{g7}-13mer antigenic peptide complexes. Within a 20-residue immunogen all possible pH 5 or 7 registers were tried, to obtain the corresponding minimised energy structures. In 36 out of 58 (62%) cases tried, the lower energy value (at pH 5 or pH 7) was obtained when a peptide was fitted into the groove in the register fulfilling the motif concordant with the ambient pH of the I-A^{g7} molecule ($p < 0.07$ by the chi-squared test). In 9 out of 58 (16%) cases the energy differences were non-significant and in 13 out of 58 (22%) cases they correlated with the discordant binding register.

The complexes of several established antigens with I-A^{g7} yielded minimised energy values that are mostly consistent with the existence of two pH-dependent motifs at p6 and p9 (Table 1). In particular, the four decamers/dodecamers from mouse and equine myoglobin [amino acids (aa) 69–78] and mouse and sperm whale myoglobin [aa 110–121] contained only pH 7 motif sequences (one or more) but not a single pH 5 motif sequence. In 7 out of 8 cases these complexes had significantly lower energies at pH 7 than at 5, also in agreement with the existence of pH-dependent motifs (Table 1). In the immunisation of NOD mice and in proliferation studies of primed lymph node T-cells with these peptides [46, 47], their binding to I-A^{g7} would not be through the endosome but at the cell membrane (ambient pH of 7.4). We conclude that the motifs already reported [21, 22], derived from binding and proliferation studies performed at specific pH values (5 or 7, respectively), generally reflect the respective preferences at pockets 6 and 9 at the given pH values, as shown by the majority of our energy calculations.

The shape of pocket 9 at endosomal and extracellular pH. Pocket 9 of the I-A^{g7} molecule is composed of residues $\alpha 68$ His, $\alpha 69$ Asn, $\alpha 72$ Ile, $\alpha 73$ Leu, $\alpha 76$ Arg, $\beta 9$ His, $\beta 30$ Tyr, $\beta 37$ Tyr, $\beta 57$ Ser and $\beta 61$ Tyr (Fig. 1, 3). The substitution of $\beta 61$ Trp (near-universally conserved among MHC II alleles) for Tyr and the absence of a $\beta 57$ Asp make for a slightly more spacious p9 pocket compared to other I-A alleles. At the endosomal pH (5.0–5.5), this pocket contains three positively charged residues, $\beta 9$ His, $\alpha 68$ His and $\alpha 76$ Arg and has another two positively charged residues, $\beta 55$ Arg and $\beta 56$ His, in its immediate vicinity (Fig. 3A). Because of the extensive electrostatic repulsions in pocket 9 at pH 5, the oppositely positioned $\alpha 76$ Arg and $\beta 57$ Ser are 2 Å further apart than at pH 7, when the groove is occupied by a peptide in the pH 7 motif register (Table 3). Our modelling showed that in all peptides fitted in the pH 5 motif register, the carboxyl group from a p9Asp/Glu would strongly interact with the $\alpha 76$ Arg and less so with the $\beta 57$ Ser side-chains and thus not penetrate much into p9 (Fig. 3, Table 3). This arrangement would also counteract the electrostatic repulsions among these five positively charged residues of pocket 9. The distance between $\beta 9$ His and the terminal carboxylate from a p9Asp/Glu at pH 5 is 9–11 Å (Table 3). At endosomal pH water molecules would probably fill this space [14, 15]. Therefore, $\beta 9$ His would be exposed to solvent and become unprotonated at extracellular pH (see below).

At neutral pH there is only one positive charge in pocket 9, from $\alpha 76$ Arg, and one close to it, that of $\beta 55$ Arg (Fig. 3B). Thus, the interaction energy between the acidic residue at p9 and nearby positively charged residues of I-A^{g7} is considerably decreased

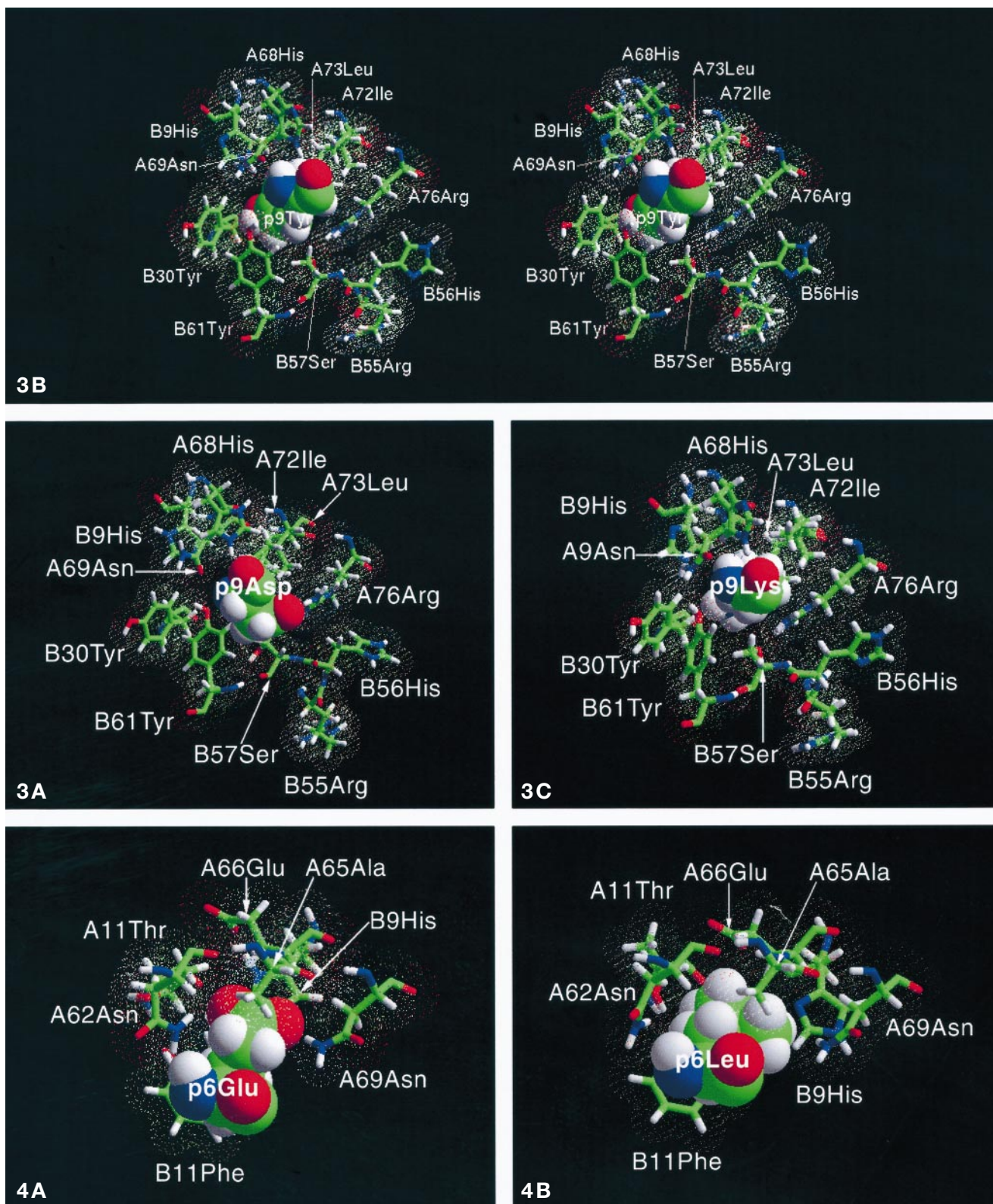


Fig. 3 A-C. The shape of pocket 9 seen in mono (**A**, **C**), or stereo (**B**) representation, with residue p9 in space filling mode and the residues from I-A^{B7} forming the pocket in stick and van der Waals dot surface representation. **A** At pH 5, containing the Asp residue of peptide 12 from murine hsp60. Residue β 37Tyr is not shown, as it is mostly covered by residue p9 in the angle at which all three pictures of pocket 9 were taken. The orientation of acidic residues in p9 at pH 5 is essentially the same in all cases of antigenic peptides of Table 1 bearing such a residue. **B** At neutral pH with the Tyr20 residue of HEL. At endosomal pH, besides the positively charged histidines at α 68, β 9 and β 56, there

are also two positively charged arginines (α 76 and β 55). There is a distinctly different orientation of β 55Arg and β 56His at pH 7, because of the absence of electrostatic repulsions between β 56His and β 55Arg or α 76Arg. At pH 7 the four preferred residues (Arg, Lys, Phe and Tyr) penetrate equally well into the p9 pocket, interacting with the proximal aromatic amino acids β 30Tyr and β 37Tyr by hydrogen bonding, π -cation, van der Waals and (in the case of Phe/Tyr) aromatic-aromatic, interaction mechanisms. **C** The fitting of p9Lys residue 534 from peptide 35 of mouse GAD65, i.e. from sequence 524–536, in pocket 9 at pH 7

Table 3. Distances (in Å) between various interacting atoms in pocket 9

| Molecule | Residue/ Atom | $\alpha 76\text{Arg}$ | | $\beta 9\text{Val}$ | | $\beta 9\text{His}$ | | $\beta 30\text{Tyr}$ O η | $\beta 37\text{Tyr}$ O η | $\beta 30\text{Tyr}$ | $\beta 37\text{Tyr}$ |
|--|--------------------------------|-----------------------|------------|---------------------|----------------|---------------------|------------------|----------------------------------|----------------------------------|----------------------|----------------------|
| | | N $\eta 1$ | N $\eta 2$ | C $\gamma 1^a$ | C $\gamma 2^a$ | N $\delta 1^b$ | N $\epsilon 2^b$ | | | | |
| I-A ^d | $\beta 57\text{Asp/O}\delta 1$ | 3.17 | 3.35 | | | | | | | | |
| I-A ^d | $\beta 57\text{Asp/O}\delta 2$ | 3.27 | 4.33 | | | | | | | | |
| I-A ^d | p9Ala/C β | | | 9.65 | 10.58 | | | | | | |
| I-A ^k | $\beta 57\text{Asp/O}\delta 1$ | 3.84 | 3.01 | | | | | | | | |
| I-A ^k | $\beta 57\text{Asp/O}\delta 2$ | 2.69 | 3.33 | | | | | | | | |
| I-A ^k | p9Ser/O γ | | | | | 8.19 | 6.87 | | | | |
| I-A ^{g7} -HEL10–22 (pH 7) | $\beta 57\text{Ser/O}\gamma$ | 2.94 | 3.86 | | | | | | | | |
| I-A ^{g7} -HEL10–22 (pH 7) | p9Tyr/O η | | | | | 6.51 | 4.59 | 5.84 | 2.54 | | |
| I-A ^{g7} -HEL10–22 (pH 7) | p9Tyr/aromatic Cs | 4.66–5.03 | 4.09–5.32 | | | | | | | 4.42–8.25 | 3.71–8.16 |
| I-A ^{g7} -mGAD 524–536 (pH 7) | $\beta 57\text{Ser/O}\gamma$ | 2.85 | 3.84 | | | | | | | | |
| I-A ^{g7} -mGAD 524–536 (pH 7) | p9Lys/N ζ | | | | | | 6.13 | | | 4.18–5.86 | 4.61–7.09 |
| I-A ^{g7} -hsp60 peptide 12 (pH 5) | $\beta 57\text{Ser/O}\gamma$ | 5.19 | 6.00 | | | | | | | | |
| I-A ^{g7} -hsp60 peptide 12 (pH 5) | p9Asp/O $\delta 1$ | 3.08 | 2.64 | | | 13.37 | 11.52 | | | | |
| I-A ^{g7} -hsp60 peptide 12 (pH 5) | p9Asp/O $\delta 2$ | 2.91 | 3.89 | | | 11.7 | 9.75 | | | | |

Values for the distances between $\beta 57\text{SerO}\gamma$ and $\alpha 76\text{ArgN}\eta 1/\text{N}\eta 2$, and $\beta 9\text{HisN}\delta 1/\text{N}\epsilon 2$ and the terminal atoms of the p9 residue are typical of what is obtained after minimisation with peptides fitted in the pH 5 or the pH 7 register with the minimisation done at the concordant pH

Data of I-A^d are from 1iad.pdb, and of I-A^k from 1iak.pdb, whereas all the data for I-A^{g7}-peptide complexes are from our own energy minimisations as described in Materials and methods

^a Refers to I-A^d only

^b Refers to I-A^k and I-A^{g7} only

(Table 1). Modelling of the fit of the high affinity HEL10–22 peptide and several of its variants in the neutral pH register indicates that Phe/Arg/Lys also fit well in p9, yielding low total energy values whereas non-favoured residues show the opposite (Table 1). Note that with a p9Arg/Lys/Phe/Tyr there is deeper penetration into the p9 pocket, additional hydrogen bonds and many van der Waals contacts between such p9 residues and the various I-A^{g7} residues constituting the p9 pocket, in contrast to the situation at pH 5 with an acidic residue at p9 (Table 3).

We examined in detail the structure of p9 of I-A^{g7} at pH 7 for an explanation of the unique Arg/Lys/Phe/Tyr selectivity of this pocket [16]. The orientation of the positively charged end of a p9Arg/Lys in the models of I-A^{g7} at pH 7 allows maximum interaction with the aromatic ring of $\beta 37\text{Tyr}$ and less so of $\beta 30\text{Tyr}$ (Fig. 3C, Table 3). This situation is identical to the π -cation interactions observed with the aromatic amino acids Tyr/Phe/Trp and positively charged Arg/Lys residues that contribute greatly to the binding between the respective groups [49]. In addition, the aliphatic parts of $\alpha 72\text{Ile}$ and $\alpha 73\text{Leu}$ come in close contact with the aliphatic portions of the p9Arg/Lys side-chain, as well as the p9Phe/Tyr aromatic ring, thus increasing the van der Waals contacts

and the stability of the complex. The binding of Phe/Tyr at p9 is also stabilised by a π -cation interaction between such residues and $\alpha 76\text{Arg}$, as the distances between the interacting groups indicate (Table 3).

Another possible contributory factor to the aromatic preference at p9 is the presence of an extensive interacting network of seven aromatic amino acids. The array of $\beta 11\text{Phe}$, $\beta 30\text{Tyr}$, $\beta 37\text{Tyr}$, $\beta 47\text{Tyr}$, $\beta 60\text{Tyr}$, $\beta 61\text{Tyr}$ and $\beta 67\text{Tyr}$ would be further stabilised by the presence of a Phe/Tyr at p9. The centre of each of these aromatic residues is less than 7 Å away from at least one centre of another aromatic residue (Table 3, Fig. 3B), the cut-off distance for interactions of this type [50].

The interaction of the two crucial residues of pocket 9, $\alpha 76\text{Arg}$ and $\beta 57\text{Ser}$, is important to the stability of the MHC II-peptide complex [9–15]. In the crystal structures of I-A^k and I-A^d, both of which exhibit the $\beta 57\text{Asp}-\alpha 76\text{Arg}$ salt bridge at this interphase, the various interatomic distances between interacting groups are small. In I-A^{g7} at pH 7 with a Phe/Tyr/Arg/Lys occupying p9 the corresponding distances are increased by 15–40% whereas at pH 5 and with an acidic residue in p9 the distances are further increased (Table 3). Thus, interactions at the p9 junction become progressively weaker from I-A^k/I-A^d to I-A^{g7} both at pH 7 and pH 5 because their energy is inversely proportional to the first and higher powers of the separating distances ([51], see Discussion).

Fig. 4A, B. The shape of pocket 6 of I-A^{g7} at **A** pH 5, containing the 517Glu residue of mouse GAD65 peptide 34 (aa510–522) and **B** neutral pH containing the 17Leu residue of HEL10–22. Carbon: green, oxygen: red, nitrogen: blue, hydrogen: white, sulphur: yellow. Representations of antigenic and pocket residues as in Fig. 3

The structure of pocket 6 at endosomal and extracellular pH. Pocket 6 of I-A^{g7} is bounded by $\alpha 11\text{Thr}$, $\alpha 62\text{Asn}$, $\alpha 65\text{Ala}$, $\alpha 66\text{Glu}$, $\alpha 69\text{Asn}$, $\beta 9\text{His}$ and $\beta 11\text{Phe}$, of which $\alpha 66\text{Glu}$ and $\beta 9\text{His}$ are ionisable. The crystal structures of I-A^d ($\beta 9\text{Val}$) and I-A^k

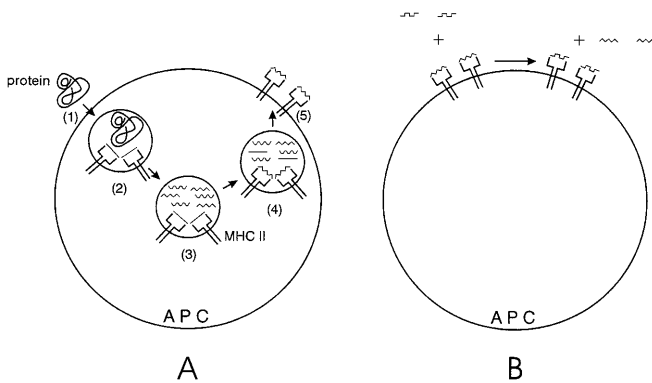


Fig. 5 A, B. Because I-A^{g7} is shown to have two different peptide-binding motifs, one at pH 5 and another at pH 7, that differ in their selectivity at p6 and p9, a difference in antigenicity could be evident between peptide and protein antigens. **A** Whole proteins are endocytosed by APCs (1), brought to the endosomal compartment (2), processed by proteolytic enzymes into peptides 15–22 residues long [16] (3); these peptides (---: Sawtooth, ~~~: Sineware), provided they fulfil the binding motif, are exchanged with CLIP (—) in the groove of MHC class II proteins at about pH 5–5.5 (part 4) and the complexes end up on the cell membrane (5), bathed by the extracellular medium with a pH of 7.4. The possibility of dissociation and rebinding is discussed in the text and shown in Fig. 6 for HEL8–22. Thus, epitopes arising from intracellularly processed proteins must satisfy the pH 5 motif to be loaded onto I-A^{g7} at the endosome, and the pH 7 motif to remain bound at the cell membrane, a condition mostly satisfied in different registers. **B** Free peptides (either injected into animals or given in vitro) that satisfy the pH 7 motif alone, can simply displace weakly bound peptides from I-A^{g7} at the cell surface [63], if they are themselves of higher affinity. This is probably best illustrated by the myoglobin nonamer and decamer peptides that contain only a pH 7 motif (Table 1)

(β9His) show the β9 residue to be part of pocket 6 as well as pocket 9 [14, 15]. Likewise, our modelling shows that β9His of I-A^{g7} also participates in the formation of pocket 6 and interacts with the p6 residue. In particular, at pH 5 the positively charged β9His interacts with the negatively charged α66Glu (Fig. 4A), an interaction that probably determines the selectivity at p6, i.e. acidic/polar residues (Table 1). By contrast, at pH 7, the now uncharged β9His turns away from α66Glu and towards α76Arg (Fig. 4B). Thus, at pH 7 pocket 6 would no longer favour the binding of acidic residues. Instead, aliphatic residues could interact well with α11Thr, α65Ala and β11Phe and are therefore favoured as shown from the energy minimisation studies (Table 1, Fig. 4B).

Discussion

We have presented a structural modelling analysis of the pH-dependence of the binding preferences at pockets 6 and 9 of I-A^{g7}, the unique MHC class II molecule of NOD mice and chief genetic component

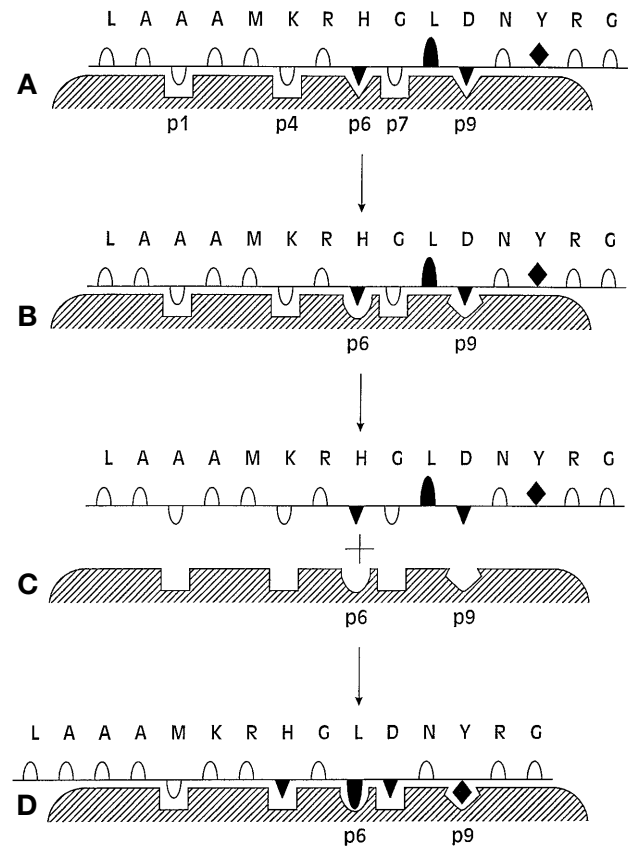


Fig. 6 A-D. The effect of pH-dependent motif changes on transition of the I-A^{g7} molecule from endosomal to extracellular pH. As pockets 1, 4, and 7 seem not to change in selectivity from one pH to the other, we depict them as indifferent (Δ) whereas pockets 6 and 9 accommodate mostly acidic residues at endosomal pH (▼). At extracellular pH pocket 6 prefers an aliphatic residue (▲) whereas pocket 9 accommodates aromatic or positively charged bulky residues (◆). The example depicted is that of HEL8–22 peptide. **A** Loading of HEL8–22 onto I-A^{g7} in the endosome with 15His at p6 and 18Asp at p9. **B** The change in pH (7.4) at the cell membrane, alters the architecture of pockets 6 and 9 that consist of one or more ionisable histidines ($pK_a = 6.0$). **C** As the HEL8–22 peptide does not fit well at pH 7 in this register, the peptide dissociates from I-A^{g7}. **D** The peptide can fit into the groove at pH 7 in a register shifted by two residues to the right, i.e. with 17Leu at p6 and 20Tyr at p9. There are few peptides with residues that show intermediate affinity at p6 and p9 both at pH 5 and pH 7 and fit well at p1, p4 and p7, which could remain attached to I-A^{g7} at pH 7 in the register bound at pH 5. Many more peptides loaded onto I-A^{g7} in the endosome do not fulfil the pH 7 motif, hence dissociate from this MHC II allele at the cell surface, leading to its observed instability in vivo. It is possible that the free peptide will exchange with a complex as in **B** because this conformation of I-A^{g7} is receptive for higher affinity binding [63]

of Type I diabetes in this model [1–3]. Homology modelling methods for prediction of protein structure are usually very successful when the modelled and the base protein have a greater than 40% amino acid identity and similar biochemical function [52]. The HIV-1 protease has been successfully modelled

Table 4. Comparison of residue preferences at various pockets at pH 5 and 7^a

| Binding character of residue at each pocket | p1 | | p4 | | p6 | | p7 | | p9 | |
|---|-----------------------|-----------------------|-------|-----------------|-------------|-------------------------|------|---------------------------|---------------|-------------------------|
| | pH 5 | pH 7 | pH 5 | pH 7 | pH 5 | pH 7 | pH 5 | pH 7 | pH 5 | pH 7 |
| wl.t. ^b | A,E,K, L,Q,T, Y | A,D,K, L,M,Q, Y | A,L,Y | A,H,K, L,Q,Y | A,E,T | I,L,M, V | L,R | A,D,E, K,L,P, Q,R,Y | A,E | F,K,R, Y |
| wk.t. ^b | R | P | K,Q,T | D,P | K,L,Q, Y | D,F,H, K,N,T, Y | A,K | | K,L,M, Q,T | D,H,L, M,N,Q, W |
| n.t. ^b | | | E | | | A,E,G, P,Q,R, S,W | | | Y | A,E,G, I,P,S, T,V |

^a Data from references 21 and 22, with permission from the authors and the publishers

^b wl.t.: well tolerated ($IC_{50} < 1 \mu\text{mol/l}$), wk.t.: weakly tolerated ($IC_{50} = 1-10 \mu\text{mol/l}$), n.t.: not tolerated ($IC_{50} > 10 \mu\text{mol/l}$) for binding to purified I-A^{g7} (pH 7 motif, [22]). For motif testing

by competitive peptide binding and proliferation of a T cell line (pH 5 motif, [21]); wl.t.: residues causing $\geq 50\%$ inhibition, wk.t.: causing 10–50% inhibition, n.t.: causing $< 10\%$ inhibition

Table 5. Consideration of binding of polyalanine peptide and HEL10–22 variants to I-A^{g7} in a different register

| Alignment of reference 22 | IC_{50} (nmol/l) ^a | Alternative alignment shifted by two positions to the left ^b |
|---------------------------|---------------------------------|---|
| Anchor position: | | |
| 1 4 6 9 | | 1 4 6 9 |
| KAAALAAYA | 50 | KAAALAAYA |
| AAAALAAYA | 50 | AAAALAAYA |
| AAAAALAAY | 25 | AAAAALAAY |
| AAAALAAY | 200 | AAAALAAY |
| AAAMKRHGLDNYRG | 300 | AAAMKRHGLDNYRG |
| AAAMKRHGLDNYR | 300 | AAAMKRHGLDNYR |
| AAAMKRHGLDNY | 150 | AAAMKRHGLDNY |
| AAAMKRHGLDN | 15,000 | AAAMKRHGLDN |

Putative anchors at p1, p4, p6, p7 and p9 in bold

^a As reported in [22] for binding to purified I-A^{g7} at pH 7.0, after permission from the publisher and authors

^b Alignment arising as suggested [60] to explain the data of reference 22

on its Rous Sarcoma Virus acid protease relative while having only 33% amino acid identity. Furthermore, this modelling was sufficiently accurate around the active site of the HIV-1 protease (where homology to acid proteases was even higher), to allow for the designing of very potent inhibitors to the enzyme [52]. The identity between I-A^{g7} and the base protein I-A^k is more than 87% in any domain, thus the modelled structures obtained should be highly similar to the actual ones, particularly as these two molecules share the crucial $\beta 65-66$ deletion. Peptide binding and homology modelling studies of mouse and human MHC class II proteins have shown results consistent with the view that HLA-DQ and I-A alleles resemble very much the fold shown in the crystal structures of the homologous (55–65% identity) proteins HLA-DR and I-E [53–57]. These studies also explain well the selective binding of given residues from antigenic peptides to specific pockets of the HLA-DQ/DR and I-A/I-E molecules, such as the exclusion of acidic residues from p4 of DRB1*0402 [12], the pref-

erences for acidic residues at p4/p7 and tryptophan at p9 of DQ2 [55, 56] and for acidic residues at p1 of I-A^k [57] and at p4 of I-E^{g7} [58].

Our energy calculations, like all other modelling studies, do not consider bound water molecules. Water molecules act as hydrogen bond bridges between the antigenic peptide backbone and the MHC II protein [11, 14]. Use of water molecules in the minimisation process did not seem feasible in the program used. The use of version 97 of the QUANTA-CHARM program (MSI, San Diego, Calif., USA) allowed us to place ten layers of water molecules over the antigen binding groove of HLA-DR1, obtaining better agreement with experimental data for the binding of peptides to DR1 (Papandreou, van Endert, Eliopoulos and Papadopoulos, unpublished results). There still is, however, no reliable approach for treating the interactions of water molecules with MHC-peptide complexes.

The allele-specific motif of I-A^{g7} has the remarkable property of different specificities at neutral and

endosomal pH, at pockets 6 and 9, as also reported from two previous independent experimental studies [21, 22]. Our modelling studies, with practically all established antigenic peptides of the NOD mouse in complex with I-A^{g7}, verify the pH selectivity of p6 and p9 of this MHC class II allele as manifested in the lower energy values of most complexes with I-A^{g7} in the concordant register ($p < 0.07$). For the peptides showing lower minimised energy at the discordant pH, or no significant energy difference between the two pH values, there could be other contributory factors to such binding, e.g. favourable interactions at the other pockets and interactions of particular “upward-pointing” peptide residues with amino acids of I-A^{g7} (haemagglutinin p5His to α 61Gln of I-A^d, HEL53Tyr to water I-A^k etc., [14–15]). Our physico-chemical analysis attributes this unique selectivity at p6 and p9 to the combination of β 9His, β 56His and β 57Ser. No other MHC II allele has more than one of these three substitutions [6, 7]. The histidine residues in pockets 6 and 9 are positively charged at pH 5 and uncharged at pH 7, altering considerably the preferences at these two pockets. In particular, β 9His is found pointing towards α 66Glu at pH 5 and towards α 76Arg at pH 7 (Fig. 4). This flipping of β 9His by 180° has also been considered for I-A^k [14].

These pH-dependent changes in residue selectivity at specific pockets have not been reported for any MHC class II allele, in contrast to differences in peptide affinity at pH 5 and 7 [59]. The latter concern pH-sensitive interactions of the peptide backbone with select MHC II residues [11]. The possibility of misalignment of the registers by either of the two I-A^{g7} motif studies (e.g. preferences at p9 and p6 of [22] match those at p7 and p4, respectively of [21]), as suggested [60], is ruled out by three considerations.

Firstly, there is general agreement about the preferred residues in pockets 1, 4 and 7 (Table 4). Secondly, although a shift by two positions to the left would match some of the preferences, it would contradict several others (Table 4). Thirdly, a shifting of the binding register of the pH 7 motif by two positions to the left would leave some of the truncated peptide variants of HEL10–22 and the polyalanine-substituted peptides in the pH 7 binding studies without any residues at p8 and p9, despite their high affinity (IC_{50} values from 25 to 300 nmol/l), a highly unlikely possibility, not reported for any MHC class II allele thus far (Table 5).

Consistent with the above, when decamer/undecamer peptides from HEL10–22 were tested for binding to purified I-A^{g7} molecules at pH 7, only the sequences 12–21 and 12–20, that fulfil the pH 7 motif, bound to I-A^{g7} (IC_{50} of 1.00 and 1.25 μ mol/l, respectively; [22]). The sequence 9–18 that contains only the pH 5 motif would not bind at all (IC_{50} equal to or greater than 15 μ mol/l, respectively; [22]). These results are consistent with our own energy calculations.

Additionally, the same group has found that a HEL10–22-specific, I-A^{g7}-restricted T-cell hybridoma responded only to the presence of the HEL12–21 peptide (p10 residue is necessary for T-cell recognition [22]) and not to the HEL9–18 or 9–19 peptides [22]. In a previous study [28], immunisation of NOD mice with intact HEL resulted in sensitised T-cells that would proliferate to many overlapping HEL peptides containing the pH 7 motif (aa12–20) but to none containing only the pH 5 motif (aa10–18). As the peptide in such proliferation assays is added exogenously (pH 7.4), the above results are strong evidence that at extracellular pH the HEL10–22 peptide binds to I-A^{g7} in one register only: with 12Met as its p1 anchor and 20Tyr its p9 anchor, i.e. fulfilling the pH 7 motif but not at all the pH 5 motif, as has been shown by us here. Furthermore, the fact that the immunogenic 69–78 and 110–120 myoglobin peptides have no pH 5 motif within their sequences but at least two pH 7 motifs, is additional evidence that the pH 7 motif is the one used by free peptides binding to I-A^{g7} on APCs in vivo and in vitro at extracellular pH.

In view of our results, three other binding studies deserve comment. In the first two, the proliferation of two different I-E α 52–68-specific and I-A^{g7}-restricted T-cell hybridomas was tested by having the mouse albumin peptide and its variants [19], or the native I-E α peptide and its variants [27], compete for binding to cognate APCs, at extracellular pH. The first of these established a requirement for acidic residues at the peptide’s carboxy-terminus [19]. The second found that a peptide containing the T-cell contact residues and a backbone of alanines bound to I-A^{g7} and stimulated the T-cells. This latter peptide shows lower total energy at pH 7 according to our calculations (Table 1). Because at pH 7 our results allow for p9Asp in some peptides and Ala is tolerated in nearly all pockets except p6 at the same pH, the conclusions of these two studies are not at variance with what is shown here. In the third study, the binding of various peptides to purified I-A^{g7} at pH 5 and 7.4 was tested, as well as the selectivity of the allele for various residues at p9 [26]. The results at pH 5 are in agreement with previous studies [19, 21, 23] showing preference for an acidic residue at p9 and with our energy calculations regarding the murine CLIP, serum albumin and transferrin peptides. However, in the competitive binding studies to I-A^{g7} at pH 7.4, the competitor peptide was used at about 5% saturation, making the drawing of any conclusions difficult.

Two modelling studies of I-A^{g7}, both based on the structure of DR1, were published [20, 21] before the pH 7 motif [22] was available. In one [21] β 57Ser interacted with the p9 acidic residue whereas β 56His pointed into the solvent and was considered as non-participating in the selectivity of pocket 9. In the other [20], modelling of I-A^{g7} showed a fitting for two antigenic peptides into the groove without testing for

particular residue preferences at p6 and p9. Our previous modelling study based on DR1, using the pH 5 and pH 7 motifs [48], found results similar to these reported here, yet certain interchain interactions were missed. Also certain structural features of I-A molecules, such as the β -bulge at α 9a and the β 84a insertion [14, 15], were not known at the time of these studies.

Our results indicate that the I-A^{g7}-peptide complexes at pH 5 with the peptide in the pH 5 motif register have greater interatomic distances at the crucial p9 junction of α 76Arg- β 57Ser, than corresponding complexes at pH 7 (Table 3). The importance of the p9 α 76Arg- β 57Asp junction to the peptide affinity of MHC class II alleles has been shown repeatedly [9–13, 16, 61]. As the interaction energies depend on $1/r$ (for charged groups), $1/r^2$ (for charged-polar group interactions), and $1/r^3$ (for polar group interactions), r being the distance between interacting groups, the increased distances would result in lower interaction energies and thus lower affinity, for I-A^{g7}-peptide complexes at endosomal pH (typical energy values for these interactions in closely spaced groups are 60, 3.6 and 0.5 kcal/mol, respectively [51]). Therefore the shorter distances between various residues around p9 at pH 7 would strengthen these interactions, leading to higher affinity binding. This conclusion is consistent with the results reported in the literature. Specifically, four binding studies at pH 4.5 to 5.5 showed binding curves with deduced dissociation constant (K_d) values of I-A^{g7} for various peptide antigens in the range of 2 to well over 100 μ mol/l (except the albumin peptide K_d of about 100 nmol/l) [18, 24–26]. Of the two binding studies done at pH 7/7.4, one reported IC_{50} values leading to K_d s for native and synthetic peptide antigens ranging from 0.05 to 30 μ mol/l [22] but in the other study such values, albeit for different peptides, were in the low to middle μ mol/l range [26]. Even then, the interaction of I-A^{g7} with certain antigenic peptides could be weak. For example, the activation of three I-A^{g7}-restricted T-cell hybridomas and a T-cell line, each specific for a different antigen required the continuous presence of the antigen [18, 26]. There was no such requirement in an I-A^k-restricted hybridoma [18]. The T-cell activation was achieved in such cases because the required serial triggering of T-cell receptors after recognition of peptide-MHC complexes is accomplished even when the free peptide concentration is well below the IC_{50} value for binding of the peptide to the MHC protein [18, 22, 26, 62].

The majority of peptide-I-A^{g7} complexes have lower energies when in the concordant pH motif register, which means that such peptides derived from endocytosed proteins in the endosome of APCs would probably dissociate at the cell surface (pH 7.4). If the peptide fulfils within its processed length a pH 7 motif, it is possible to rebind in the latter regis-

ter. We consider it noteworthy that all peptide epitopes arising from immunisation of NOD mice with whole proteins contain both a pH 5 and a pH 7 motif within their naturally processed length [63] (Fig. 5 and 6). This is not the case for peptide immunisation, as exemplified by the myoglobin peptides (Table 1).

Because of the lower concentration of dissociated peptide in extracellular space compared with that in the endosomal compartment, the percentage of such newly formed I-A^{g7}-peptide complexes would be low. Thus, there would be a rapid turnover of I-A^{g7} molecules at the cell surface. In addition, the I-A^{g7}-peptide complexes are of lower affinity due to weaker p9 interactions compared with β 56Pro β 57Asp⁺ alleles. Consequently, I-A^{g7} would be unstable to SDS treatment in vivo [18, 28–31] and in vitro [18, 26]. Such stability does not always correlate with high-affinity peptide binding [64] but in general this is considered to be the case [65]. From this viewpoint, our documentation of weaker expected affinities of I-A^{g7} to peptides is consistent with the instability of this allele to SDS. Only one laboratory has shown SDS-stability of such complexes [21, 23], a discrepancy possibly arising from the different procedure used by this group; specifically, the incubation of the immunoprecipitated I-A^{g7} molecules with the high affinity hsp60 peptide 12 at a high final concentration (200 μ mol/l) at pH 5, before SDS treatment. This procedure would lead to SDS-stable complexes.

The existence of a pH 5 and a pH 7 motif for p6 and p9 of I-A^{g7} (as shown by us here) and the low to medium affinity with which this allele generally binds to peptides at either pH, lead to pH-dependent differences in peptide affinity, possible dissociation and probable rebinding in a different register and to low apparent stability at the cell membrane. Because of such unique properties there would be relatively few high affinity I-A^{g7}-peptide combinations that would result in negative selection in the thymus. The latter process would operate in NOD mice at a much higher threshold of peptide affinity than it does in most other mouse strains. Therefore, the NOD mouse would have a higher than normal number of positively selected I-A^{g7}-restricted autoreactive CD4⁺ T-cells emerging from the thymus. This hypothesis has already been put forth to explain experimental findings in NOD mice [46, 66] and further evidence has been provided by another laboratory [67].

The results of our modelling also provide a possible explanation of the protection from diabetes of NOD mice transgenically expressing modified I-A^{g7} or other MHC class II alleles [2, 4, 24, 68]. In all such cases the transgenically expressed MHC II molecule has a pH-invariant motif, with a higher peptide affinity and MHC II-peptide stability, due to the absence of β 56His or presence of β 57Asp or both. The transgenically expressed MHC II allele could eliminate or suppress the generation of diabetogenic CD4⁺ T-cells

by “determinant capture” or “repertoire skewing” or any other regulatory mechanism(s) [2, 24, 28, 68–72]. Such mechanisms have been shown in NOD mice to depend on the ratio of transgene/I-A^{g7} expression on APCs in the thymus and the periphery [36, 68–70].

In extrapolating our results to human Type I diabetes, it should be kept in mind that in humans the role of the β 57 residue along with other subtle points in the structure of susceptible and resistant HLA-DQ alleles is paramount [2, 8, 57, 73], as the β 9His- β 56His- β 57Ser combination is unique to I-A^{g7}.

Acknowledgements. G.K. Papadopoulos dedicates this work to his doctoral adviser, Professor Joseph Y. Cassim, Emeritus, of the Doctoral Program in Biophysics and the Department of Microbiology at The Ohio State University, Columbus, Ohio, USA, for teaching him the importance of structure to biological function.

This work was supported in part by a Biotech grant to G.K. Papadopoulos from the European Union (contract no. BIO4 CT95 0263) and a supplementary grant from the Hellenic Secretariat of Research and Technology. G.K. Papadopoulos wishes to thank Dr. E. Eliopoulos for his invaluable help in teaching him the fundamentals of the Silicon Graphics Indy workstation as well as the Biosym/MSI software. We also wish to thank Dr. H.-G. Rammensee for unpublished information that confirmed our insights into I-A^{g7}, and Dr. C. Bartsocas for his encouragement and support.

This work was presented in part at the 5th Biannual Meeting of the Hellenic Diabetes Association, Athens, March 1997 and the 34th Meeting of the European Association for the Study of Diabetes, Barcelona, Spain, September 1998 [ref. 48].

Note Added in proof: Very recent binding studies to I-A^{g7} at pH 6 via phage display libraries have shown the pH 7 motif to be the predominant one [74]. Also, “empty” MHC class II molecules have been demonstrated on the cell membrane of mouse immature dendritic cells [75]; this, in concert with newly found extracellular proteolytic activities from such cells, raise new possibilities for antigen presentation in immune responses.

References

1. Kikutani H, Makino S (1992) The murine autoimmune diabetes model: NOD and related strains. *Adv Immunol* 51: 285–322
2. Tisch R, McDevitt H (1996) Insulin-dependent diabetes mellitus. *Cell* 85: 291–297
3. Wicker LS, Todd JA, Peterson LB (1995) Genetic control of autoimmune diabetes in the NOD mouse. *Annu Rev Immunol* 13: 179–200
4. Nishimoto H, Kikutani H, Yamamura K-i, Kishimoto T (1987) Prevention of autoimmune insulinitis by expression of I-E molecules in NOD mice. *Nature* 328: 432–434
5. Acha-Orbea H, McDevitt HO (1987) The first external domain of the nonobese diabetic mouse class II I-A β chain is unique. *Proc Natl Acad Sci USA* 84: 2435–2439
6. Kabat EA, Wu TT, Reid-Miller M, Perry HM, Gottesman KS (1991) Aminoacid sequences of proteins of immunological interest, (5th edn). NIH, Bethesda
7. Marsh SGE (1998) HLA Class II region sequences, 1998. *Tissue Antigens* 51: 467–507 (Also at the net site <http://www.anthonynolan.org.uk/HIG/>)
8. Todd JA, Bell JI, McDevitt HO (1987) HLA-DQ β gene contributes to susceptibility and resistance to insulin-dependent diabetes mellitus. *Nature* 329: 599–604
9. Stern LJ, Brown JH, Jardetzky TS, Gorga JC, Urban RG, Strominger JL, Wiley DC (1994) Crystal structure of the human class II MHC protein HLA-DR1 complexed with an influenza virus peptide. *Nature* 368: 215–221
10. Ghosh P, Amaya M, Mellins E, Wiley DC (1995) The structure of an intermediate in class II MHC maturation: CLIP bound to HLA-DR3. *Nature* 378: 457–462
11. Fremont DH, Hendrickson WA, Marrack P, Kappler J (1996) Structures of an MHC Class II molecule with covalently bound single peptides. *Science* 272: 1001–1004
12. Dessen A, Lawrence CM, Cupo S, Zaller DM, Wiley DC (1997) X-ray crystal structure of HLA-DR4 (DRA*0101, DRB1*0401) complexed with a peptide from human collagen II. *Immunity* 7: 473–481
13. Smith KJ, Pyrdol J, Gauthier L, Wiley DC, Wucherpfennig KW (1998) Crystal structure of HLA-DR2 (DRA*0101, DRB1*1501) complexed with a peptide from human myelin basic protein. *J Exp Med* 188: 1511–1520
14. Fremont DH, Monnaie D, Nelson CA, Hendrickson WA, Unanue ER (1998) Crystal structure of I-A^k in complex with a dominant epitope of lysozyme. *Immunity* 8: 305–317
15. Scott CA, Peterson PA, Teyton L, Wilson IA (1998) Crystal structures of two I-A^d-peptide complexes reveal that high affinity can be achieved without large anchor residues. *Immunity* 8: 319–329
16. Rammensee H-G, Friede T, Stevanovic S (1995) MHC ligands and peptide motifs: first listing. *Immunogenetics* 41: 178–228 (Also at the net site: <http://www.uni-tuebingen.de/uni/kxi/>)
17. Klein J (1986) Natural history of the major histocompatibility complex. John Wiley, New York
18. Carrasco-Marin E, Shimizu J, Kanagawa O, Unanue ER (1996) The class II MHC I-A^{g7} molecules from non-obese diabetic mice are poor peptide binders. *J Immunol* 156: 450–458
19. Reich E-P, von Grafenstein H, Barlow A, Swenson KE, Williams K, Janeway CA Jr (1994) Self peptides isolated from MHC glycoproteins of non-obese diabetic mice. *J Immunol* 152: 2279–2288
20. Amor S, O’Neill JK, Morris MM et al. (1996) Encephalitogenic epitopes of myelin basic protein, proteolipid protein, and myelin oligodendrocyte glycoprotein for experimental allergic encephalomyelitis induction in Biozzi ABH (H-2A^{g7}) mice share an aminoacid motif. *J Immunol* 156: 3000–3008
21. Reizis B, Eisenstein M, Bockova J et al. (1997) Molecular characterization of the diabetes-associated mouse MHC class II protein, I-A^{g7}. *Int Immunol* 9: 43–51
22. Harrison LC, Honeyman MC, Trembleau S, et al. (1997) A peptide binding motif for I-A^{g7}, the class II Major Histocompatibility Complex (MHC) molecule of NOD and Biozzi AB/H mice. *J Exp Med* 185: 1013–1021
23. Reizis B, Altmann DM, Cohen IR (1997) Biochemical characterization of the human diabetes-associated HLA-DQ8 allelic product: similarity to the major histocompatibility complex class II I-A^{g7} protein of non-obese diabetic mice. *Eur J Immunol* 27: 2478–2483
24. Chao C-C, Sytwu H-K, Chen EL, Toma J, McDevitt HO (1999) The role of MHC class II molecules in susceptibility to type I diabetes: Identification of peptide epitopes and characterization of the T cell repertoire. *Proc Natl Acad Sci USA* 96: 9299–9304
25. Xu X-J, Gearon C, Stevens E, Vergani D, Baum H, Peakman M (1999) Spontaneous T-cell proliferation in the non-

- obese diabetic mouse to a peptide from the unique class II MHC molecule, I-A^{E7}, which is also protective against the development of autoimmune diabetes. *Diabetologia* 42: 560–565
26. Hausmann DHF, Yu B, Hausmann S, Wucherpfennig KW (1999) pH-dependent peptide binding properties of the type I diabetes-associated I-A^{E7} molecule: rapid release of CLIP at an endosomal pH. *J Exp Med* 189: 1723–1733
 27. Carrasco-Marin E, Kanagawa O, Unanue ER (1999) The lack of consensus for I-A^{E7}-peptide binding motifs: Is there a requirement for anchor amino acid side chains? *Proc Natl Acad Sci USA* 96: 8621–8626
 28. Deng H, Apple R, Clare-Salzler M et al. (1993) Determinant capture as a possible mechanism of protection afforded by major histocompatibility complex class II molecules in autoimmune disease. *J Exp Med* 178: 1675–1680
 29. Carrasco-Marin E, Kanagawa O, Unanue ER (1997) Insights into the chemistry and biology of the I-A^{E7} class II molecule. *Res Immunol* 148: 291–301
 30. Nabavieh A, Chou H, Volokhov I et al. (1998) Development of an I-A^{E7}-expressing antigen-presenting cell line: intrinsic molecular defect in compact I-A^{E7} dimer generation. *J Autoimmun* 11: 63–71
 31. Peterson M, Sant AJ (1998) The inability of the nonobese diabetic class II molecule to form stable peptide complexes does not reflect a failure to interact productively with DM. *J Immunol* 161: 2961–2967
 32. Baekkeskov S, Aanstoot H-J, Christgau S et al. (1990) Identification of the 64K autoantigen in insulin-dependent diabetes as the GABA-synthesizing enzyme glutamic acid decarboxylase. *Nature* 345: 151–156
 33. Kaufman DL, Clare-Salzler M, Tian J et al. (1993) Spontaneous loss of T-cell tolerance to glutamic acid decarboxylase in murine insulin-dependent diabetes. *Nature* 366: 69–72
 34. Tisch R, Yang X-D, Singer SM, Liblau RS, Fugger L, McDevitt HO (1993) Immune response to glutamic acid decarboxylase correlates with insulinitis in non-obese diabetic mice. *Nature* 366: 72–75
 35. Chen S-L, Whitley PJ, Freed DC, Rothbard JB, Peterson LB, Wicker LS (1994) Responses of NOD congenic mice to a glutamic acid decarboxylase-derived peptide. *J Autoimmun* 7: 635–641
 36. Hanson MS, Cetkovic-Cvrlje M, Ramiya VK et al. (1996) Quantitative thresholds of MHC class II I-E expressed on hemopoietically-derived antigen-presenting cells in transgenic NOD/Lt mice determine level of diabetes resistance and indicate mechanism of protection. *J Immunol* 157: 1279–1287
 37. Quinn A, Sercarz EE (1996) T cells with multiple fine specificities are used by non-obese diabetic (NOD) mice in response to GAD(524–543). *J Autoimmun* 9: 365–370
 38. Chao C-C, McDevitt HO (1997) Identification of immunogenic epitopes of GAD 65 presented by A^{E7} in non-obese diabetic mice. *Immunogenetics* 46: 29–34
 39. Cetkovic-Cvrlje M, Gerling IC, Muir A, Atkinson MA, Elliott JF, Leiter EH (1998) Retardation or acceleration of diabetes in NOD/Lt mice mediated by intrathymic administration of candidate β -cell antigens. *Diabetes* 46: 1975–1982
 40. Zechel MA, Elliott JF, Atkinson MA, Singh B (1998) Characterization of novel T-cell epitopes on 65 kDa and 67 kDa glutamic acid decarboxylase relevant in autoimmune responses in NOD mice. *J Autoimmun* 11: 50–62
 41. Boyton RJ, Lohmann T, Londei M et al. (1998) Glutamic acid decarboxylase T lymphocyte responses associated with susceptibility or resistance to type 1 diabetes: analysis in disease discordant human twins, non-obese diabetic mice and HLA-DQ transgenic mice. *Int Immunol* 10: 1765–1776
 42. Tisch R, Wang B, Serreze DV (1999) Induction of glutamic acid decarboxylase 65-specific Th2 cells and suppression of autoimmune diabetes at late stages of disease is epitope dependent. *J Immunol* 163: 1178–1187
 43. Tian J, Lehmann PV, Kaufman DL (1994) T cell cross-reactivity between Coxsackievirus and glutamate decarboxylase is associated with a murine diabetes susceptibility allele. *J Exp Med* 180: 1979–1984
 44. Daniel D, Gill RG, Schloot N, Wegmann DR (1995) Epitope specificity, cytokine production profile and diabetogenic activity of insulin-specific T cell clones isolated from NOD mice. *Eur J Immunol* 25: 1056–1062
 45. Zekzer D, Worg FS, Wen L et al. (1997) Inhibition of diabetes by an insulin-reactive CD4 T-cell clone in the non-obese diabetic mouse. *Diabetes* 46: 1124–1132
 46. Ridgway WM, Fassò M, Lanctot A, Garvey C, Fathman CG (1996) Breaking self-tolerance in nonobese diabetic mice. *J Exp Med* 183: 1657–1662
 47. Ridgway WM, Fathman CG (1998) The association of MHC with autoimmune diseases: understanding the pathogenesis of autoimmune diabetes. *Clin Immunol Immunopathol* 86: 3–10
 48. Papadopoulos GK (1998) Homology modeling of I-A^{E7} verifies the existence of two peptide binding motifs (pH 5 and pH 7) explains several properties of this MHC II allele from NOD mice. *Diabetologia* 56: 101A (Abstract)
 49. Dougherty DA (1996) Cation- π interactions in chemistry and biology: a new view of benzene, Phe, Tyr and Trp. *Science* 271: 163–168
 50. Burley SK, Petsko GA (1985) Aromatic-aromatic interaction: a mechanism of protein structure stabilization. *Science* 229: 23–28
 51. Atkins PW (1998) *The Elements of Physical Chemistry*, (2nd edn). Oxford University Press, Oxford, pp 377–378
 52. Weber IT (1991) Modeling of structure of Human Immunodeficiency Virus-1 protease with substrate based on crystal structure of Rous Sarcoma Virus protease. *Methods Enzymol* 202: 727–741
 53. Sanjeevi CB, Lybrand TP, DeWesee C et al. (1995) Polymorphic amino acid variations in HLA-DQ are associated with systematic physical property changes and occurrence of IDDM. *Diabetes* 44: 125–131
 54. Paliakasis K, Routsias J, Petratos K, Ouzounis C, Kokkinidis M, Papadopoulos GK (1996) Novel structural features of the human histocompatibility molecules HLA-DQ as revealed by modeling based on the published structure of the related molecule HLA-DR1. *J Struct Biol* 117: 145–163
 55. Vartdal F, Johansen BH, Friede T et al. (1996) The peptide binding motif of the disease associated HLA-DQ ($\alpha 1^*0501, \beta 1^*0201$) molecule. *Eur J Immunol* 26: 2764–2772
 56. van de Wal Y, Kooy YMC, Drijfhout JW, Amons R, Papadopoulos GK, Koning F (1997) Peptide-binding features of the disease-associated DQ($\alpha 1^*0501, \beta 1^*0201$) molecule versus the non-disease-associated DQ($\alpha 1^*0201, \beta 1^*0202$) allele. *Immunogenetics* 46: 484–492
 57. Nelson CA, Viner NJ, Young SP, Petzol SJ, Unanue ER (1996) A negatively charged anchor residue promotes high affinity binding to the MHC class II molecule I-A^k. *J Immunol* 157: 755–762
 58. Gregori S, Trembleau S, Penna G et al. (1999) A binding motif for I-E^{E7}, the MHC class II molecule which protects NOD-E α transgenic nonobese diabetic mice from autoimmune diabetes. *J Immunol* 162: 6630–6640
 59. Jensen PE (1991) Enhanced binding of peptide antigen to purified class II Major Histocompatibility glycoproteins at acidic pH. *J Exp Med* 174: 1111–1120

60. Reizis B, Eisenstein M, Mor F, Cohen IR (1998) The peptide binding strategy of the MHC class II I-A molecules. *Immunol Today* 19: 212–216
61. Marshall KW, Liu AF, Canales J et al. (1994) Role of polymorphic residues in HLA-DR molecules in allele-specific binding of peptide ligands. *J Immunol* 152: 4946–4957
62. Valitutti S, Muller S, Cella M, Padovan E, Lanzavecchia A (1995) Serial triggering of many T-cell receptors by a few peptide-MHC complexes. *Nature* 375: 148–151
63. Natarajan SK, Assadi M, Sadegh-Nasseri S (1999) Stable peptide binding to MHC class II molecule is rapid and is determined by a receptive conformation shaped by prior association with low affinity peptides. *J Immunol* 162: 4030–4036
64. Verreck FA, Vermeulen C, Poel AV et al. (1996) The generation of SDS-stable HLA-DR dimers is independent of efficient peptide binding. *Int Immunol* 8: 397–404
65. Nelson CA, Petzold SJ, Unanue ER (1994) Peptides determine the life span of MHC class II molecules in the antigen-presenting cell. *Nature* 371: 250–252
66. Kim DT, Rothbard JB, Bloom DD, Fathman CG (1996) Quantitative analysis of T cell activation. Role of TCR/ligand density and TCR affinity. *J Immunol* 156: 2737–2742
67. Kanagawa O, Martin SM, Vaupel BA, Carrasco-Marin E, Unanue ER (1998) Autoreactivity of T cells from non-obese diabetic mice: An I-A^{g7}-dependent reaction. *Proc Natl Acad Sci USA* 95: 1721–1724
68. Parham P (1990) A diversity of diabetes. *Nature* 345: 662–664
69. Schmidt D, Verdaguer J, Averill N, Santamaria P (1997) A mechanism for the major histocompatibility complex-linked resistance to autoimmunity. *J Exp Med* 186: 1059–1075
70. Ridgway WM, Ito H, Fassò M, Yu C, Fathman CG (1998) Analysis of the role of variation of major histocompatibility complex class II expression on nonobese diabetic (NOD) peripheral T cell response. *J Exp Med* 188: 2267–2275
71. Nepom GT (1990) A unified hypothesis for the complex genetics of HLA associations with IDDM. *Diabetes* 39: 1153–1157
72. Schmidt D, Amrani A, Verdaguer J, Bou S, Santamaria P (1999) Autoantigen-independent deletion of diabetogenic CD4⁺ thymocytes by protective MHC class II molecules. *J Immunol* 162: 4627–4636
73. Routsias J, Papadopoulos GK (1995) Polymorphic structural features of modelled HLA-DQ molecules segregate according to susceptibility or resistance to IDDM. *Diabetologia* 38: 1251–1261
74. Gregori S, Bono E, Gallazzi F, Hammer J, Harrison LC, Adorini L (2000) The motif for peptide binding to the insulin-dependent diabetes mellitus-associated class II MHC molecule I-A⁹⁷ validated by phage display library. *Intl Immunol* 12: 493–503
75. Santambroglio L, Sato AK, Carven GJ, Belyanskaya SL, Strominger JL, Stern LJ (1999) Extracellular antigen processing and presentation by immature dendritic cells. *Proc Natl Acad Sci USA* 96: 15056–15061